Optica Applicata, Vol. X, No. 4, 1980

Directional Selective Cover for Solar Energy Concentrators

MUNAIM A. MASHKOUR

Department of Physics, College of Science, University of Mosul, Iraq.

A theoretical analysis is given here for a directional selective cover for solar energy concentrators. The cover limits the radiation exchange to within definite solid angle and suppresses the large angle emission radiation. The emission solid angle is determined by the refractive index of the cover in the infrared region $n(i)$. At $n(i) \geqslant 2.613$, which is realized by several non-oxid chalcogenide glasses, the emission solid angle can be reduced to zero, and thus there will be total suppression of infrared radiation. Considerable amplification of the concentration ratio is still attainable with refractive indices characteristic of ordinary optical glasses.

Introduction

The principal aim of all solar energy concentrators is to reduce the emission infrared radiation at a maximum collection of incoming solar radiation. To that purpose various imaging and non-imaging designs, and spectral selective coatings have been used. Yet a property which has not been fully expoloited is the directional property of the direct solar radiation, whereas the emission radiation has a wide angular distribution. Thus, if somehow the radiation exchange is limited to within a narrow solid angle, while the large angle emission radiation is suppressed, the effective emissivity of the concentrator will be reduced without affecting the collection efficiency of the direct solar radiation. Few applications of this principle have been proposed in the literature [1], where these concentrators are termed directional selective ones.

The present article is to propose a design of a directional selective cover for solar energy concentrators, which suppresses large angle emission of infrared radiation, but still admits most of the direct solar radiation. The transmission solid angle of the cover is widened along a definite direction which can be made parallel to the sun path, thus no constant diurnal tracking of the concentrator is required.

The function of the cover is based upon the total internal reflection. This property has been, in fact, previously used in designing dielectric filled compound parabolic concentrators [2]. The crucial refractive index of the cover corresponds to the emission infrared radiation: $\lambda = 1-10\ \mu$, and subsequently whenever special reference is made to this region, the symbol $n(i)$ will be used for the refractive index.

The cover may be used in conjunction with practically all flat and non-flat concentrators for direct solar radiation, where the overall con-

centration ratio, i.e. the absorbtance to emissivity ratio of the concentrator becomes the product: $(a/e)_b \times (a/e)_c$, where $(a/e)_b$ is the concentration ratio of the concentrator without the directional selective cover, and $(a/e)_c$ is the concentration ratio of the cover, i.e. its transmittance for the direct solar radiation to its effective transmittance for the emission infrared radiation from the underlying absorbing layer. The resultant concentration efficiency is also determined by a product law.

The concentration ratio $(a/e)_c$ increases sharply with the increasing refractive index $n(i)$, and a total suppression of the emission infrared radiation can be achieved at $n(i) \geqslant 2.613$. In fact, these refractive indices are realized by several non-oxid chalcogenide glasses [3]. These materials have the further relevant property where their absorption coefficient for infrared radiation is small. On the other hand, at $n(i) = 2$, the concentration ratio of the cover becomes comparable with the geometric concentration ratio of a typical compound parabolic concentrator [4]. Even at $n(i) = 1.6$, one obtains $(a/e)_c = 1.63$, which is still a considerable amplification of the concentration ratio*.

General description

The cover is made of three transparent plates, each of them is ridged from one side with ridged angle α, as in fig. 1, and the plates are arranged with the spacings, as seen in fig. 2, with the flat side facing the incident solar radiation. It is more convenient to determine the transmittance of the cover for radiation incident from its top side. The final result will be, of course, also valid for the infrared radiation coming from the bottom side of the cover.

The figure 1 shows the traces of three typical rays in the top plate, entering from its flat side: 1 — a ray which reaches an inclined interface with an incidence angle less than the critical angle for total internal reflection θ_c (ray 1). This ray will pass directly to the opposite side of the plate, where it is assumed here that no reflection takes place at these angles. This point will be reconsidered in *Discussion*. 2 — a ray which reaches an inclined interface with an incidence angle $\theta \geqslant \theta_c$, and is internally reflected toward the top interface 0 (ray 2). It can be shown that after two further internal reflections this ray will emerge from the original side of the plate, so that the ray's initial direction $\boldsymbol{l}_0$, its final direction $\boldsymbol{l}_0$, and the normal to the plate $\boldsymbol{N}$, satisfy the known laws of reflection. 3 — a ray which reaches an inclined interface with an incidence angle $\theta \geqslant \theta_c$, and is internally reflected

---

* These ratios are obtained when the underlying absorbing layer is an ideal black body. They are approximately doubled when spectral selective coating is used.

toward a next inclined interface (ray 3). This ray after two further internal reflections, will ultimately emerge from the opposite side of the plate.

In the figure 2 the rays of type 3 in the fig. 1 are suppressed by a proper choice of the ridges angle α. This case will be discussed in next section. Here, we are dealing with representative traces of five classes of rays in

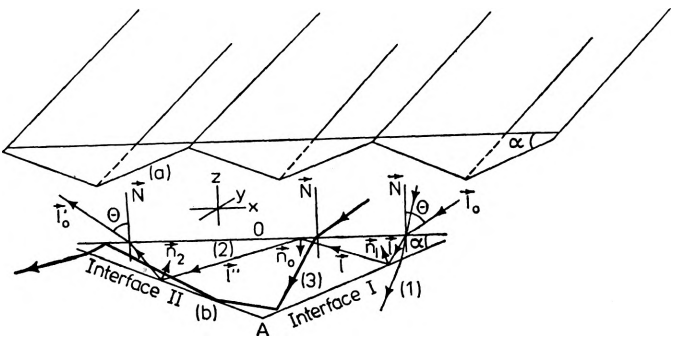

Fig. 1. a. A ridged transparent plate; b. Typical refracted rays. For simplicity the rays are drawn in the plane of the paper

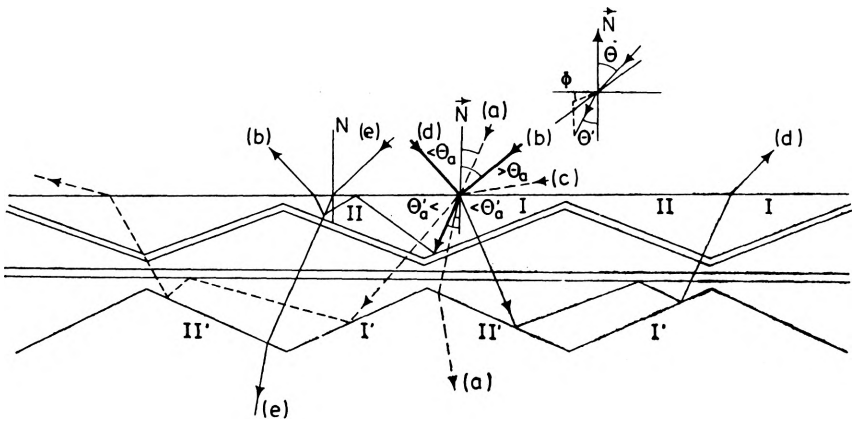

Fig. 2. Arrangement of the cover plates. The figure also shows the following typical rays: a-rays, incident close to the normal $\vec{N}$, and thus pass directly through the cover; b-, c-, and d-rays are ultimately reflected from the cover, e-rays, though incident at large angles, will leak to the opposite side of the cover

the entire plates stack, namely: a-rays, being incident close to the normal N, will pass directly through the stack. These rays will define the transmission solid angle to be discussed in section *The Transmission Solid Angle*. b-, c-, and d-rays, being incident at larger angles with the normal, follow the routes indicated in the figure. These rays will ultimately emerge back from the original side of the stack, with their initial directions, final

directions, and the normal to the plates stack, they satisfy the known laws of reflection. Finally *e*-rays, though incident at large angles, will cross to reach the opposite side of the stack. These rays comprise the stray radiation which will be considered in section *The Stray Radiation.*

The choice of the ridges angle

The performance of the cover depends to a large extend on the choice of the ridges angle a. This angle must be chosen so as:

1) to suppress the rays of type 3 in the fig. 1,

and

2) to minimize the transmission solid angle for the a-rays of the fig. 2.

Requirement 1) demands a to be not too large, while requirement 2) demands a to be as large as possible. A detailed analysis, taking into account the uniform distribution of the radiation over the entire plate, has led to the following choices:

$$a = \sin^{-1}\left(\frac{1}{n(i)}\right), \quad \text{if} \quad n(i) \geqslant 2.613 = \frac{1}{\sin 22.5^\circ}, \tag{1}$$

$$a = 22.5^\circ, \quad \text{if} \quad n(i) \leqslant 2.613. \tag{2}$$

Hence, it can be readily observed that for $n(i) \geqslant 2.613$, the transmission solid angle for infrared radiation diminishes to zero.

The transmission solid angle

The figure 2 shows that the rays which enter from the top interface will be reflected from interface I or II, provided that they make in these surfaces incidence angles greater than the critical angle for total internal reflection. The cut-off refraction angle θ'_a for a ray to be transmitted through, say, interface I, is determined by the ray's azimuthal angle Φ — relative to a direction normal to the ridges lines, the critical angle for total internal reflection θ_c, and the ridges angle a, by the relation

$$\cos\Phi = \frac{\cos\theta_c - \cos\theta'_a \cos a}{\sin\theta'_a \sin a},$$

whereas the cut-off incidence angle for the concerned transmission is

$$\theta_a = \sin^{-1}(n \sin\theta'_a). \tag{3}$$

Equation (3) defines the boundary of the transmission solid angle against the reflections from interface I. The reflections from the interface II leave the transmission solid angle which is a mirror image to the first solid angle, as in fig. 3, and the resultant transmission solid angle Ω is the intersection of the two solid angles. It is observed that the angle Ω is widened along the direction of the ridges lines.

The figure 4 shows the boundaries of the transmission solid angles for different refractive indices $n < 2.613$, using ridges angle $\alpha = 22.5°$. A compilation of the angular selectivity $S = \Omega/2\pi$, i.e. the ratio of the transmission solid angle to the total emission solid angle, is shown in table 1. The solid angles Ω have been determined by numerical evaluation of the

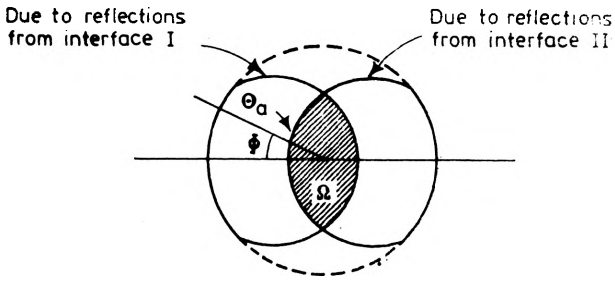

Fig. 3. The resultant transmission solid angle through the cover is the intersection of the transmission solid angle against reflections from interfaces I and II

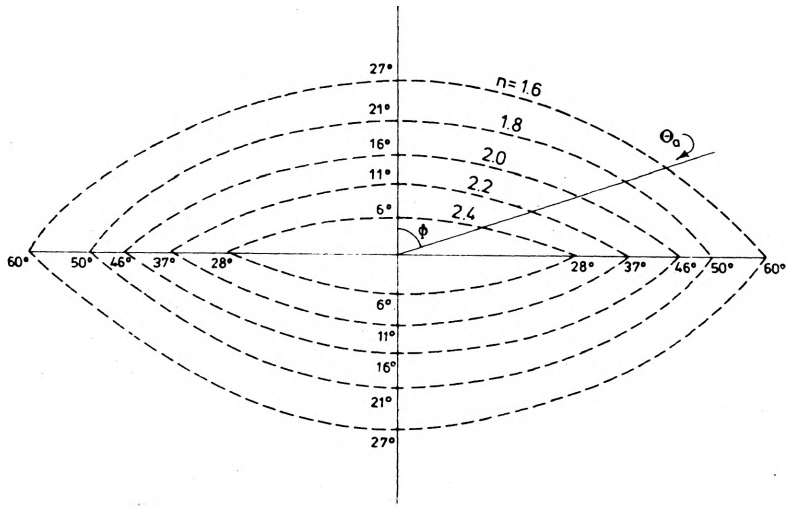

Fig. 4. The boundaries of the transmission solid angles for different refractive indices, the ridges angle $\alpha = 22.5°$

Table 1

The angular selectivity S as a function of the refractive index n

n	1.6	1.8	2.0	2.2	2.4
$S = \frac{\Omega}{2\pi}$	0.221	0.147	0.100	0.061	0.034

integral $\iint \sin\theta \, d\theta d\Phi$, with the limits of integrations given by eq. (3). Figure 5 shows the variation of the angular selectivity with the refractive index.

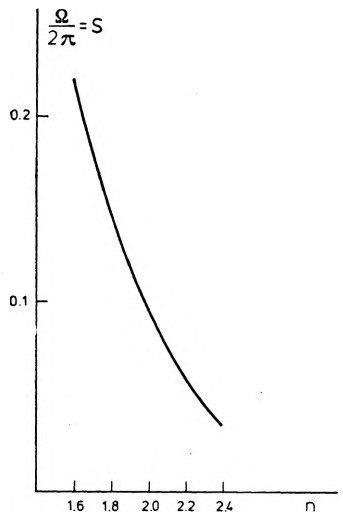

Fig. 5. The angular selectivity S as a function of the refractive index

The stray radiation

It can be seen form fig. 6 that it is possible to totally block the stray radiation (i.e. that is represented by the *e*-rays in fig. 2) from leaking across the plates stack, by using reflecting strips of half-width: $x = s \tan\theta_c = x_0$, at the positions shown in the figure, where θ_c is the critical angle for total internal reflection, and s is the ridges height. These strips, however, act to decrease the transmission efficiency od direct solar radiation, i.e. the efficiency decreases by a factor $1 - 2x/2L$, where $2L$ is the ridge width. The optimal performance of the cover requires a detailed analysis of the effect of the strips half-width on the stray radiation.

The figure 7 shows a ridge of the lower plate. It is seen that the cut-off refraction angle θ'_e for an incident ray to pass through the plates is determined by its incidence distance x and its azimuthal angle Φ by the relation: $\tan\theta'_e = \dfrac{x}{s\cos\Phi}$, whereas the cut-off incidence angle is: $\theta_e = \sin^{-1}(n\sin\theta'_e)$.

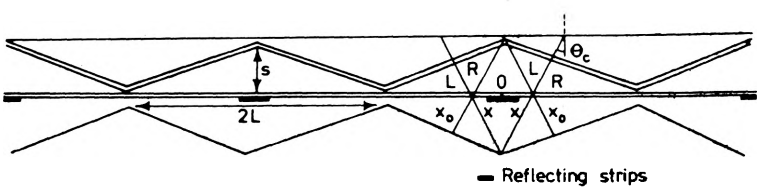

Fig. 6. Reflecting strips to eliminate stray radiation

The stray solid angle $\Omega_e(x)$ at incidence distance x is then the integral: $\Omega_e(x) = \iint \sin\theta\, d\theta\, d\Phi$, with the limits of integrations given by the above cut-off relations. On the other hand, referring back to fig. 6, the leakage factor, i.e. the effective transmittance of the cover due to crossing of the R and L rays shown in the figure, is given by

$$\mathscr{L} = \frac{4}{(2\pi)\,(2L)} \int_{x}^{x_0} \Omega_e(x')\, dx'. \tag{4}$$

This quantity has been evaluated numerically for various values of the strips half-width, and various refractive indices, and the results are presented in table 2. The figure 8 shows the variation of $\mathscr{L}$ with x/s, for

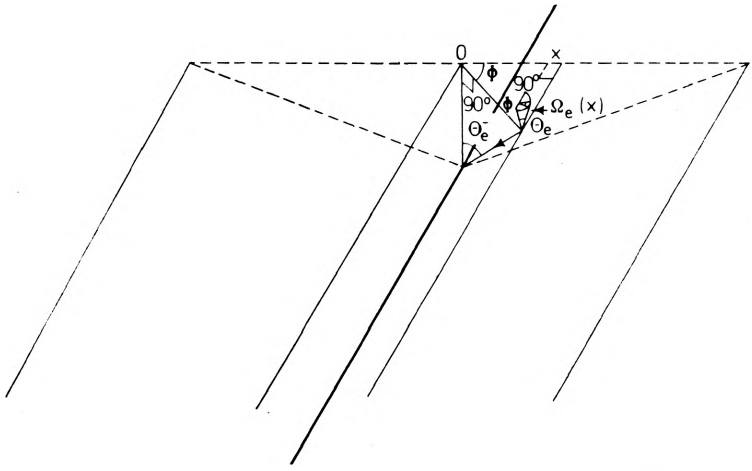

Fig. 7. The cut-off refraction angle θ_e' for the stray radiation

Table 2

The variation of the leakage factor $\mathscr{L}$ with strip half-width x, for different refractive index n; s is the ridges height

x/sn	0.0	0.1	0.2	0.3	0.4	0.5	0.6	0.7
1.6	0.1616	0.1219	0.0880	0.0592	0.0370	0.0197	0.0079	0.0020
1.8	0.1313	0.0934	0.0620	0.0368	0.0190	0.0069	0.0008	
2.0	0.1111	0.0735	0.0439	0.0233	0.0086	0.0012		
2.2	0.1009	0.0639	0.0367	0.0160	0.0040			
2.4	0.0909	0.0540	0.0099	0.0016				

different refractive indices. It is seen that the leakage factor decreases sharply with increasing half-width of the strips, while the collection effi-

ciency decreases linearly. The half-width of the strips has to be taken such that the corresponding leakage factor $\mathscr{L}$ is a small fraction of the angular selectivity S.

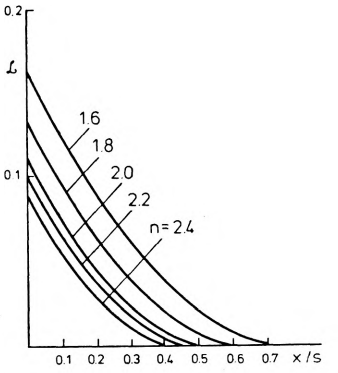

Fig. 8. The variation of the leakage factor $\mathscr{L}$ with strips half-width x, at different refractive indices

Discussion

Both the leakage factor $\mathscr{L}$ and the angular selectivity S, contribute to the transmittance of the cover for the emission infrared radiation. This transmittance is also determined by the angular distribution of the radiation. Assuming isotropic emission intensity from the underlying absorbing layer, which is approximately characteristic of a grey body, the effective transmittance of the cover for the emission infrared radiation will be:

$$e_{\text{isotropic}} = S + \mathscr{L}, \tag{5}$$

while for a cos-law emission intensity, which is characteristic of ideal black body, the effective transmittance of the cover for the emission radiation will be:

$$e_{\text{black}} = 2(S + \mathscr{L}). \tag{6}$$

In the latter case, the effective emission solid angle is $\int\int \cos\theta \sin\theta \times d\theta d\Phi = \pi$ rather than 2π. On the other hand, it has been noted that the effective transmittance of the cover for the direct solar radiation is $a = 1 - x/L$, where L and x are the ridges and reflecting strips half-widths, respectively.

From the foregoing calculations, it can be easily shown by assuming the cos-law intensity distribution that for $n(i) = 1.6$, 2.0, and 2.4, and

using reflecting strips of half-width 0.4 s (s is the ridges height) the concentration ratio of the cover $(a/e)_c$ will be equal to 1.63, 4.2, and 12.4, respectively, at collection efficency 84%. For isotropic intensity distribution the concentration ratios are doubled.

On the other hand, it has been noted in section *The choice of the ridges angle* that if $n(i) \geqslant 2.613$, and using ridges angle $\alpha = \sin^{-1}\left(\frac{1}{n(i)}\right)$, the transmission solid angle diminishes to zero. Furthermore, using reflecting strips of half-width $x = s \tan\alpha$, the stray radiation will be also totally blocked. Thus at these refractive indices complete suppression of the emission infrared radiation can be achieved. Here the effective transmittance of the cover for the direct solar radiation is: $a = \frac{n^2(i)-2}{n^2(i)-1}$.

Final remarks

1. The transmission solid angle can have different sizes for the direct solar radiation and the emission infrared radiation, depending on the refractive indices in the visible and infrared regions. These angles are widened along the direction of the ridges lines. The latter fact helps to avoid constant diurnal tracking of the concentrator, provided that the cover is installed with its ridges parallel to the sun path.

2. In all of the foregoing considerations, reflections other than the total internal reflection have been neglected. These reflections, however, affect the performance of the present cover, as well as all ordinary multiglazing covers. It may be readily realized that the inclined interfaces make negligible contribution to the effective reflectance of the cover for the radiation coming within the transmission solid angle: a ray coming within this angle and internally reflected from an inclined interface, will be turned back by a subsequent total internal reflection from a horizontal interface, so that it will proceed readily in its original direction. Only the horizontal interfaces affect the overall reflectance of the cover for this radiation. Analyses lead to the following expression for the effective transmittance of the cover for the radiation coming within the transmission solid angle: $T = \frac{(1-r)^2}{1+r-2r^2}$, where r is the reflectance of a single air-glass interface. This transmittance, evaluated in the proper spectral region, scales the foregoing geometric transmittance of the cover for the direct solar radiation a, and the emission infrared radiation e.

It is a pleasure to thank Professor Abdus Salam of the ICTP for his kind hospitality during the compilation of this paper. I also wish to thank K. Mansoor for discussions concerning the optical properties of glasses.

References

[1] HOLLANDS K. G., Solar Energy **7** (1963), 108.
[2] WINSTON R., Appl. Opt. **15** (1976), 291.
[3] HILTON A. R., Lectures on Glass Science and Technology. Delivered at the Rensselear Polytechnic Institute, Troy, N. Y. 1966.
[4] WELFORD W. T., WINSTON R., *The Optics of Nonimaging Concentrators*, Academic Press, New York 1978, p. 131.

Received August 20, 1979
in revised form March 1, 1980

Направленно селективное покрытие сгустителей солнечной энергии

Прлизведён теоретический анализ направленно селективных покрытий для сгустителей солнечной энергии. Покрытия ограничивают обмен энергии определёнными постоянными углами и подавляют излучение, испускаемое под большими углами. Пространственный угол эмиссии определяется коэффициентом преломления покрытия в инфрокрасной области спектра. При $n(i) \geqslant 2.613$, осуществляемом несколькими перексидными халькогенными стёклами пространственный угол излучения может быть уменьшен до нуля и произойдёт полное подавление инфракрасного излучения. Значительное усиление отношения концентрации является всё ещё достигаемым для коэффициентов преломления, характерных для обычных оптических стёкол.